Continental Shelf Research 31 (2011) 244–253

Contents lists available at ScienceDirect

Continental Shelf Research

journal homepage: www.elsevier.com/locate/csr

Nitrate to silicate ratio variability and the composition of micro-phytoplankton blooms in the inner-fjord of Seno Ballena (Strait of Magellan, 54°S)

Rodrigo Torres [a,*], Máximo Frangópulos [b], Madeleine Hamamé [a], Vivian Montecino [c], Constanza Maureira [d], Gemita Pizarro [b,e], Brian Reid [a], Arnoldo Valle-Levinson [f], Jose Luis Blanco [g]

[a] Centro de Investigación en Ecosistemas de la Patagonia, Bilbao 449, Coyhaique, Chile
[b] Centro de Estudios del Cuaternario Fuego-Patagonia, Avenida Bulnes 01890, Punta Arenas, Chile
[c] Departamento de Ciencias Ecológicas, Facultad de Ciencias, Universidad de Chile, Las Palmeras 3425, Casilla 653, Santiago, Chile
[d] Laboratorio de Química Marina, Centro de Investigación en Ecosistemas de la Patagonia, Bilbao 449, Coyhaique, Chile
[e] Instituto de Fomento Pesquero, Enrique Abello 0552, Punta Arenas, Chile
[f] Civil and Coastal Engineering Department, University of Florida, Gainesville, FL, USA
[g] Old Dominion University, Norfolk, VA, USA

ARTICLE INFO

Article history:
Received 24 September 2009
Received in revised form
26 July 2010
Accepted 28 July 2010
Available online 12 August 2010

Keywords:
Tidal intrusion front
N:Si ratio
Nitrate
Dissolved silicate
Fjord
Patagonia

ABSTRACT

The along-fjord variability of nitrate and dissolved silicate was studied in a silled fjord, Seno Ballena, in the Strait of Magellan during flood and ebb tidal phases in December 2007. The spatial and temporal variability of both nitrate and dissolved silicate were consistent with the dynamics of a tidal intrusion front previously described for this fjord by Valle-Levinson et al. (2006). During flood, maximum nitrate values were found seaward and close to the sill due to the upwelling of dense, nutrient-rich water by means of Bernoulli aspiration. Conversely, a sharp drop in surface nitrate landward of the sill was consistent with the sinking of saltier, nitrate-rich, dissolved silicate-poor upwelled waters under relatively less dense, nitrate-poor, dissolved silicate-rich surface waters after flowing landward over the shallow sill. The waters flooding over the sill were particularly enriched in nitrate but poor in dissolved silicate, (NO_3^-:$Si(OH)_4$ ratio $\sim$5). The ratio tended to decrease landward of the sill, particularly during the ebb tide (NO_3^-:$Si(OH)_4$ ratio <2), but the absolute $Si(OH)_4$ concentration values were still very low, normally ranging between 2 and 3 μM $Si(OH)_4$. Consistent with the low availability of dissolved silicate (DSi), only dinoflagellates (in the micro-phytoplankton size range) bloomed in nitrate-enriched (10 μM NO_3^-) waters at the base of a shallow halocline. Thus, it is likely that the variability of surface water nutrients and DSi in Seno Ballena results mainly from the interplay among tidally forced fertilization (the aspiration of subpycnocline water with a high NO_3^-:$Si(OH)_4$ ratio), the input of continental waters (low NO_3^-:$Si(OH)_4$ ratio), and local productivity. The combination of these factors explains the micro-phytoplankton composition observed landward of the sill on this and previous expeditions to the study area.

1. Introduction

Fjords, like most estuaries (Perillo, 1995), are productive aquatic systems due to the input of nutrients having both marine and terrestrial origins (Mann and Lazier, 1996). Primary producers (in the micro size range) that bloom in the fjords and channels of Chilean Patagonia are normally diatoms and dinoflagellates (e.g., Clément and Guzmán, 1989; Uribe, 1992; Iriarte et al., 1993; Hamamé and Antezana, 1999; Iriarte et al., 2001; Uribe and Ruiz, 2001; Molinet et al., 2003; Pizarro et al. 2005; Alves-de-Souza et al., 2008a; Vargas et al., 2010). Bottom-up regulatory mechanisms, particularly the amount and proportion of available nutrients and dissolved silicate, have been routinely invoked to explain the relative dominance of diatoms vs. others functional groups (e.g., Officer and Ryther, 1980; Egge and Aksnes, 1992; Conley et al., 1993; Turner et al., 1998; Allen et al., 2005).

Blooms of chain diatoms during austral spring in the Strait of Magellan (southern Patagonia; Iriarte et al., 2001) can explain the drastic reduction of both nitrate (NO_3^-) and dissolved silicate (DSi; orthosilicic acid, $Si(OH)_4$) in the water column (Antezana and Hamamé, 1999). However, in deeper subpycnocline waters, the nitrate concentration is typically higher than the DSi concentration (Antezana and Hamamé, 1999). This nutrient distribution has been observed at different times and at various Patagonian sites

* Corresponding author. Tel.: +56 67 24 4533; fax: +56 67 24 4501.
E-mail address: rtorres@ciep.cl (R. Torres).

0278-4343/$ - see front matter © 2010 Elsevier Ltd. All rights reserved.
doi:10.1016/j.csr.2010.07.014

(e.g., Braun et al., 1993; Catalano et al., 1996; Silva and Calvete, 2002; Silva and Guzman, 2006; Silva and Valdenegro, 2008).

Fertilization mechanisms involving deep mixing or the upwelling of these deep waters are expected to bring water with a high NO_3^-: $Si(OH)_4$ ratio to the surface. However, this effect (high surface water NO_3^-:$Si(OH)_4$ ratio) could be reset by the inflow of continental waters (see Dávila et al., 2002) enriched in DSi but normally poor in inorganic nitrogen (e.g., Perakis and Hedin, 2002; Silva and Guzman, 2006; Frangópulos et al., 2007; Huygens et al., 2008; Vargas et al., 2010) and by NO_3^- consumption by non-diatom dominated phytoplankton assemblages (e.g., in late summer; Magazzù et al., 1996; Iriarte et al., 2001).

Tidal forcing plays a major role in the water circulation of most Patagonian fjords and channels (e.g., Antezana et al., 1992). Topographic constrictions or sills influence the basin circulation in a variety of ways (e.g., Seim and Gregg, 1997), thereby affecting the transport of dissolved nutrients between the basins separated by the topographic feature (e.g., from a channel to a fjord). Cokelet et al. (2007) have shown particularly high nitrate enrichment over a sill in Glacier Bay, Alaska, compared to surrounding areas in the Gulf of Alaska. Although fertilization processes associated with tidal forcing may be important for determining biological production within adjacent basins, particularly after an early spring bloom, little is known about how these mechanisms affect the spatio-temporal variability of nutrients. Waters found landward of the sill, or up-fjord waters, are normally well stratified because of freshwater inflow. This characteristic vertical stratification seems to be a key factor leading to the onset of phytoplankton blooms in nutrient-replete waters (Holmedal and Utnes, 2006). Thus, hydrodynamic processes affecting the amount and proportion of nutrients in highly stratified up-fjord waters could be relevant to the onset, type, and spatial distribution of phytoplankton blooms in Patagonian fjords.

Seno Ballena (Fig. 1) is an example of the many virtually pristine and poorly known Patagonian fjord systems. Connected to the Strait of Magellan, this fjord stretches approximately 18 km in length from the face of a glacier to the strait. The inner-fjord is approximately 9 km long and typically less than 1 km wide. The lithology of the fjord is based on the Southern Patagonia Batholith, dominated by granitic rocks and downgrading to granitodiorites and gabbro in the outer third of the fjord (Servicio Nacional de Geología y Minería, 2003). In this periglacial area, sub-glacial discharges and the calving of glacial ice at the head of the fjord are expected to be the mayor source of freshwater to the fjord. Additionally the snow accumulated on top of the adjacent mountains feeds streams during warm periods, as do, possibly hundreds of more diffuse sources of freshwater cascading from the margins of the fjord during precipitation events (R. Torres, unpublished data); this many sources of freshwater provides the fjord with a thin buoyant layer (see Valle-Levinson et al., 2006).

A shallow sill (2–3 m depth) covered with *Macrocystis* kelp beds practically blocks the mean landward flow of high salinity water, which is pumped over the sill and toward the glacier only during flood tides (Valle-Levinson et al., 2006). Seno Ballena has a characteristic tidal intrusion front over the sill (Valle-Levinson et al., 2006), with denser water intruding into a basin of more buoyant water and plunging downward as a gravity current (e.g., Largier, 1992; O'Donnell, 1993). The acceleration of the flood tidal flows in the area of the sill produces the conditions necessary for suctioning deep waters (Seim and Gregg, 1997), a phenomenon known as aspiration (Stommel et al., 1973). A detailed analysis of the circulation in Seno Ballena in December 2003 and 2004 suggests that, during flood periods, deep water is aspirated to near-surface levels as the flow accelerates over the sill crest (Valle-Levinson et al., 2006). This mechanism is expected to transport subpycnocline water to the surface from an aspiration depth of ~30 m (Valle-Levinson et al., 2006) and, thus, may be a major fertilization mechanism for up-fjord waters in Seno Ballena. In order to test this hypothesis, concentrations of nitrate and DSi were measured along the axis of the fjord, crossing the sill, during flood and ebb. Additionally, the vertical distribution of nutrients, chlorophyll-a (Chl-a) in three size ranges, micro-phytoplankton abundances, and hydrographic parameters are reported.

2. Methods

In December 2007, a survey was carried out along Seno Ballena (Fig. 1). The survey included: (1) a CTD transect of seven stations along the fjord axis; (2) seawater sampling and CTD observations at four stations (P1–P4, three up-fjord and one down-fjord; Fig. 1); and (3) surface seawater sampling along a transect over the sill during flood and ebb (see Fig. 1).

The seven CTD stations (in Fig. 1, stations 1–7) were sampled with a Seabird 19 plus CTD on 16 December 2007 during the ebb tide (19:46–21:15). Additionally, at each station, surface water

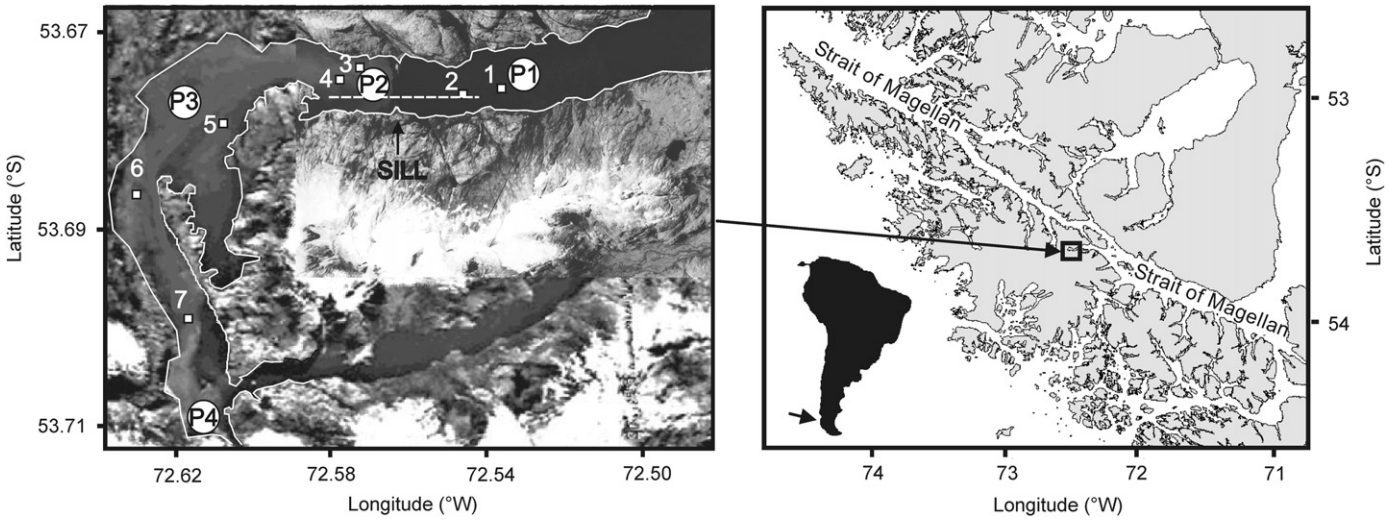

Fig. 1. Study area, left panel shows Seno Ballena Fjord. Squares depict the CTD transect (St. 1–7) and circles the approximate location of seawater sampling stations (P1–P4). The dashed line depicts the ~2-km-long transect (over the sill) where surface water was collected.

samples were collected with a bucket and poured into BOD bottles using Tygon tubing. These samples were immediately fixed and analyzed for dissolved oxygen (DO) following Dickson (1995) within 24 h after collection. We calculated the apparent oxygen utilization (AOU) following Murray and Riley (1969), based on both CTD and DO data.

Vertical seawater sampling and CTD profiling were done at four stations in the fjord (in Fig. 1, stations P1–P4). Seawater samples were taken with a suction system (an all-plastic membrane pump and polyethylene tubing); the inlet was attached to the CTD frame. Thus, we obtained relatively high vertical resolution that also matched both CTD (pressure, conductivity, temperature) and chemical data. The seawater samples were analyzed for both nutrients and Chl-a. Seawater for nitrate and silicate analyses was poured into 250-mL acid-cleaned polyethylene bottles and frozen at −24 °C until further analysis (Strickland and Parsons, 1968). For total Chl-a, 100 mL of seawater were filtered over glass fiber filters (0.5 μm nominal pore size), which were frozen (−24 °C) until later analysis by fluorometry with a Trilogy Turner Designs fluorometer calibrated with *Anacystis nidulans* (Sigma), using acetone (90% v/v) for the pigment extraction (Parsons et al., 1984).

Additionally, in order to estimate the Chl-a content in the pico, nano, and micro size fractions, 100 mL of seawater were pre-filtered through 20-μm nets and then filtered using a 2.0-μm Nucleopore filter (nano size fraction), and another 100 mL were pre-filtered through a 2.0-μm Nucleopore filter and filtered using a 0.2-μm membrane filter (pico size fraction). The relative contribution of the three size categories (pico, nano, micro) to the total Chl-a concentration was calculated for two strata: above (~0–5 m depth) and below (~9–20 m depth) the halocline. Sampling was limited to the top 20 m and the sampling depths were variable, approximately every 1 above 10 m. In the shallow zone near the glacier tip, Station P4 was sampled at two depths. At Station P3 (where Chl-a levels were highest in the micro size range, see Results), the abundance of micro-phytoplankton was determined following Utermöhl (1958), and the total biovolume (a proxy of biomass) of each major group (i.e., diatoms, dinoflagellates) was calculated based on the analogy of the shape of the phytoplankton with simple geometrical forms (Olenina et al., 2006).

Bucket samples of surface water were collected along the cross-sill transect (Fig. 1) during flood (24 stations along the transect, 17 December 2007, 18:52–19:06) and ebb (12 stations along the transect, 16 December 2007, 19:15–19:36). Vessel location (using a GPS) and bottom depth were recorded for each station sampled. The surface seawater samples were poured into 250-mL acid-cleaned, polyethylene bottles and maintained in the dark and frozen (−24 °C) until analyzing for nitrate and silicate. This was done with an FIA nutrient autoanalyzer using colorimetric methods based on Strickland and Parsons (1968). Replicates in the actual range of concentration had a mean coefficient of variation (CV) of 0.8% for NO_3^- and 0.5% for $Si(OH)_4$.

3. Results

3.1. Hydrography, nutrients, and chlorophyll along the fjord

Fragments of ice moving seaward precluded navigation near the fjord head during the CTD transect carried out during the ebb tide and moving up-fjord toward the glacier (Fig. 1). At the end of the transect (St. 7, near the glacier; Fig. 2a), the top 3 m showed uniform low temperatures. The vertical salinity gradient was highest in the top 4 m (Fig. 2b) and, as expected, water density was governed by salinity (Fig. 2c). Both density and salinity were higher at the outer (St. 1, 2) than at the inner fjord stations (St. 3–7) (Fig. 2b–c).

The surface water temperature decreased toward the glacier (Fig. 3), surface density and salinity were substantially high at the outer stations, and DO increased toward the glacier where the surface water was colder. The AOU indicated that most stations were slightly supersaturated in DO, with the exception of the station near the up-fjord side of the sill (St. 3); this station was also characterized by the lowest salinity (and density) and the highest surface temperature (Fig. 3).

The vertical sampling coupled to CTD profiling (Fig. 4) showed that, in the top 20 m, nitrate levels ranged from 0.2 to 12 μM NO_3^-. Nitrate was low in surface waters near the glacier (St. P4; Fig. 4). Subpycnocline waters (> 10 m depth) had higher levels of nitrate at inner-fjord stations (i.e., St. P2, P3; ~12 μM NO_3^-) than at the outer-fjord station (St. P1 had a maximum of ~10 μM NO_3^-; Fig. 4). Dissolved silicate levels ranged from ~1 to ~5 μM $Si(OH)_4$ (Fig. 4). Dissolved silicate and nitrate were not correlated ($p > 0.05$). The NO_3^-:$Si(OH)_4$ ratio ranged from 0 to 9; however, at depths > 10 m, this ratio ranged from 2 to 6. The NO_3^-:$Si(OH)_4$ ratio of the deepest sample taken at Station P1 (deep waters that can be aspirated during flood tide) was ~4.

The Chl-a vertical distribution showed a sharp subsurface maximum at 2–5 m depth, corresponding approximately to the base of the halocline-pycnocline (see dashed line in Fig. 4). Above 5 m, most Chl-a was represented by the picoplankton size fraction at stations P1, P2, and P4 (60%, 64%, and 60%, respectively; Fig. 5). Station P3 was an exception, with most Chl-a contained in the microplankton size fraction (58%). Below 10 m depth (subpycnocline water), the contribution of picoplankton to Chl-a levels decreased and the nanoplankton contribution increased at the inner-fjord stations, particularly Station P3 (79%). Maximum inner-fjord Chl-a levels (St. P3) corresponded to a dinoflagellate bloom (Fig. 6). Dinoflagellate biovolume (Fig. 6a) was larger than diatom biovolume at all depths, particularly at 3 m depth, where dinoflagellate abundance was the highest (Fig. 6b) and dominated by *Scrippsiella* sp. (Fig. 6c).

3.2. Variability of surface nitrate and DSi over the sill during flooding and ebbing

During flood, the surface water that entered the inner fjord was enriched in nitrate (Fig. 7a) and poor in DSi (Fig. 7b). During ebb, in contrast, the surface water leaving the inner-fjord was enriched in DSi (Fig. 7b) and low in nitrate (Fig. 7a).

3.2.1. Nitrate and DSi over the sill during flood

During flood, surface nitrate was low (5.7 ± 0.1 μM NO_3^-, $n=8$) and relatively constant (coefficient of variation, CV = 1%) along the up-fjord or inner portion of the transect (Fig. 7; positive values on the *x*-axis). Over the down-fjord or outer portion of the transect, however, nitrate concentrations were substantially higher (9.1 ± 0.3 μM NO_3^-, $n=14$) and slightly more variable (CV = 4%). The concentration of surface water nitrate along the outer portion of the transect decreased from the sill towards the Strait of Magellan (i.e., surface water nitrate and the distance from the sill were inversely correlated; $R=-0.8$, $p<0.05$, $n=14$; Table 1).

The concentration of DSi in the surface water was relatively high along the inner portion of the transect (2.9 ± 0.1, $n=8$, CV = 3%) compared to the outer portion (2.1 ± 0.1, $n=14$, CV = 5%). The surface water DSi increased from the sill towards the Strait of Magellan, that is, surface water DSi and the distance from the sill were correlated ($R=0.9$, $p<0.05$, $n=14$; Table 1; Fig. 7).

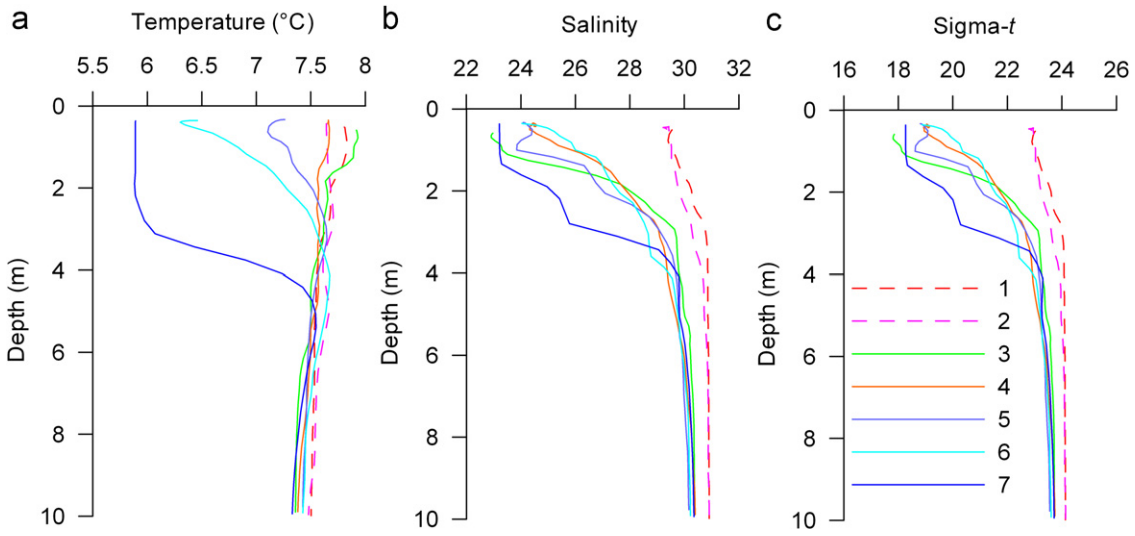

Fig. 2. CTD profiles along Seno Ballena Fjord during ebbing (December 2007). Continuous and dashed lines depict CTD profiles for the outer and inner-fjord, respectively.

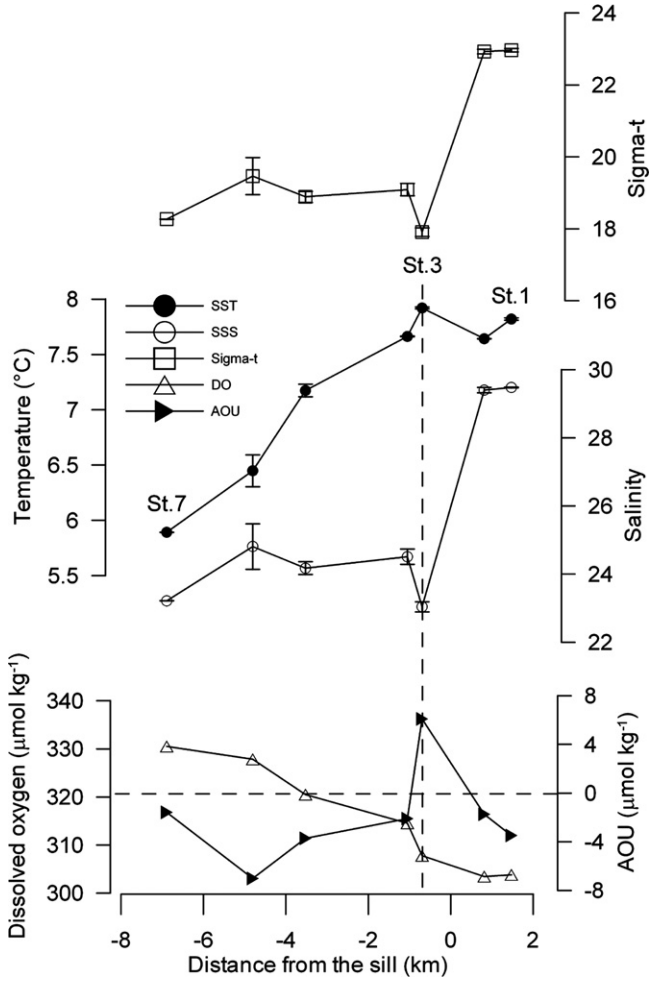

Fig. 3. Surface water properties (top 1 m depth) along Seno Ballena Fjord in December 2007. SST: sea surface temperate; SSS: sea surface salinity; DO: dissolved oxygen; AOU: apparent oxygen utilization. Vertical dashed line depicts St. 3 location. Horizontal dashed line depicts dissolved oxygen saturation level.

3.2.2. Nitrate and DSi over the sill during ebb

During ebb, surface nitrate was 5.1 ± 0.1 µM NO_3^- ($n=4$, CV=3%) along the inner portion of the transect and slightly higher along the outer transect (5.4 ± 0.1 µM NO_3^-, $n=14$, CV=4%). Surface water nitrate and the distance from the sill were not correlated during ebb (Table 1; Fig. 7). Surface nitrate was lowest over the sill (shallow depth; ~2 m depth). Surface silicate was 3.4 ± 0.1 µM $Si(OH^-)_4$ ($n=4$, CV=3%) along the inner portion of the transect and slightly lower along the outer portion, where nitrate was higher (3.2 ± 0.1 µM $Si(OH^-)_4$, $n=14$, CV=7%). The maximum surface silicate levels were observed over the sill (Fig. 7).

3.3. Nitrate and DSi fluxes across the sill

In order to calculate nitrate and silicate fluxes, current velocity data collected in the vicinity of the shallow sill (Valle-Levinson et al., 2006, 2007) were used to determine volume fluxes (in cubic meters per second). Interactions of tidal flows with the shallow sill caused marked distortions in the tidal signal (Valle-Levinson et al., 2007) and also in the tidal fluxes (Fig. 8a). Positive transports were seaward. Maximum tidal transports reached 400 $m^3 s^{-1}$ during ebb but, on average, they were around 200 $m^3 s^{-1}$ during ebb V_{out} and near 125 $m^3 s^{-1}$ during flood V_{in}. Through conservation of mass ($V_{out}=V_{in}+R$), the freshwater discharged R to the fjord was around 80 $m^3 s^{-1}$.

The tidal fluxes shown in Fig. 8a were used to compute nitrate fluxes by assuming concentrations of 5 during ebb and 9 µM during flood. Even though these concentrations would be expected to change within each phase of the tide, Fig. 7 shows that concentrations seaward and landward of the sill changed little, with a drastic change appearing within a very short distance over the sill. Therefore, temporal changes of concentrations on both sides of the sill should be expected to be rather small and the assumption of constant concentrations during each phase of the tide is likely adequate. The net nitrate flux estimated in this way (Fig. 8b) yields a value of –0.5 moles s^{-1} directed into the inner-fjord. Moreover, the net nitrate flux obtained by assuming zero concentration during ebb and 9 µM during flood is –0.8 moles s^{-1} into the inner-fjord. Similarly, the net silicate flux determined with a concentration of 3.1 µM, invariant during ebb, and 2.1 µM, constant during flood (Fig. 8c), is +0.03 moles s^{-1} toward the ocean, out of the inner-fjord.

4. Discussion

4.1. Surface water nutrient variability in Seno Ballena

A previous study of the hydrography of Seno Ballena suggests that, during flood periods, deep water is aspirated from subpycnocline

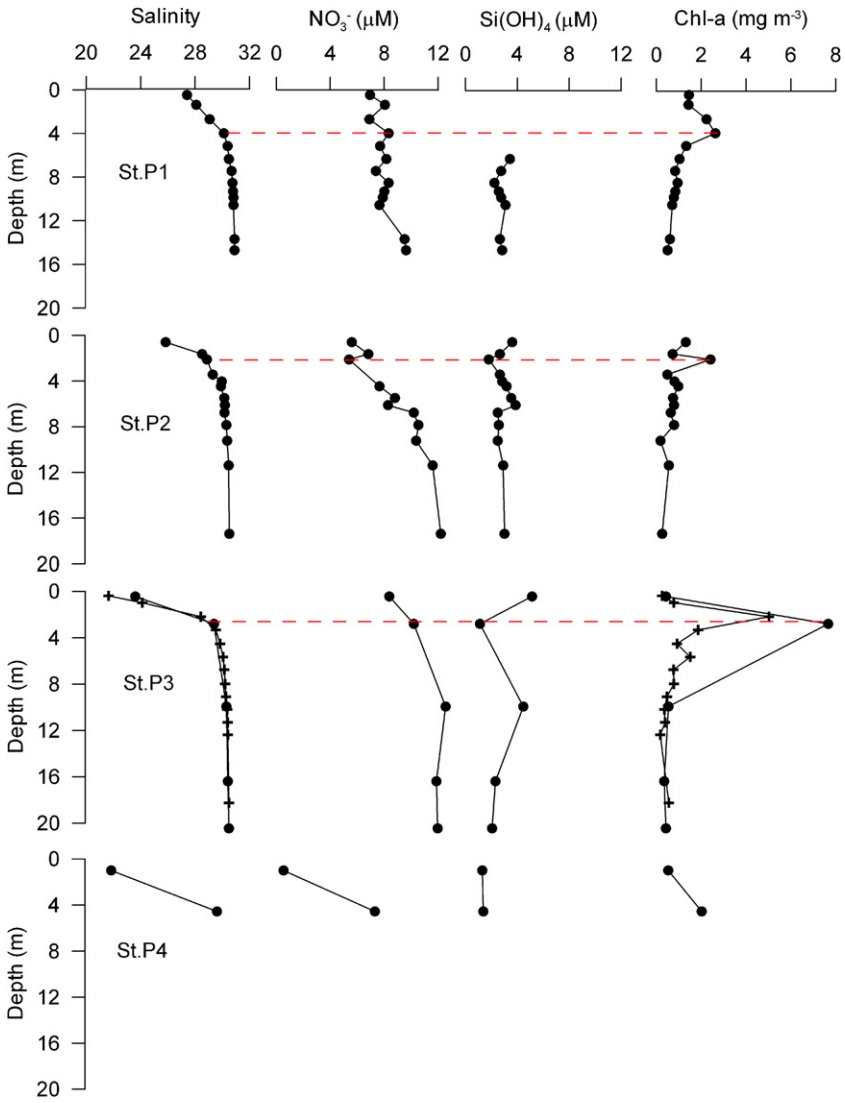

Fig. 4. Vertical profiles of salinity, nitrate, DSi, and Chl-a along Ballena Fjord in December 2007. The dashed lines indicate the location of the Chl-a maximum.

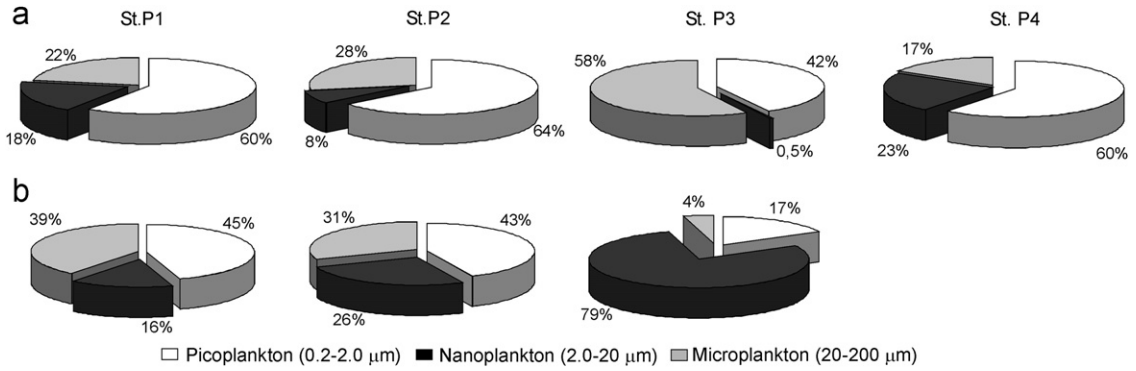

Fig. 5. Chl-a content in the pico, nano, and micro size fractions taken above (a) and below (b) the pycnocline/halocline in Ballena Fjord in December 2007.

layers on the external side of the sill (Valle-Levinson et al., 2006). Consistent with this, we observed the highest surface nitrate concentration (~10 μM NO_3^-) on the external side of the sill during flood (Fig. 7). These maximum surface levels were similar to nitrate levels observed in subpycnocline waters during ebb (~10 μM NO_3^- at St. P1; Fig. 4). Indeed, the surface nitrate decreased seaward (from the sill; Table 1) only for this period (flood) and location, indicating that the maximum nitrate fertilization was specifically associated with the sill during flood (see Fig. 7). The surface nitrate levels observed at this location (~10 μM NO_3^-) were near the maximum values reported for the euphotic layer in the Strait of Magellan (e.g., Braun et al., 1993; Saggiomo et al., 1994; Catalano et al., 1996; Vanucci and Mangoni, 1999; Iriarte et al., 2001; Frangópulos et al., 2007).

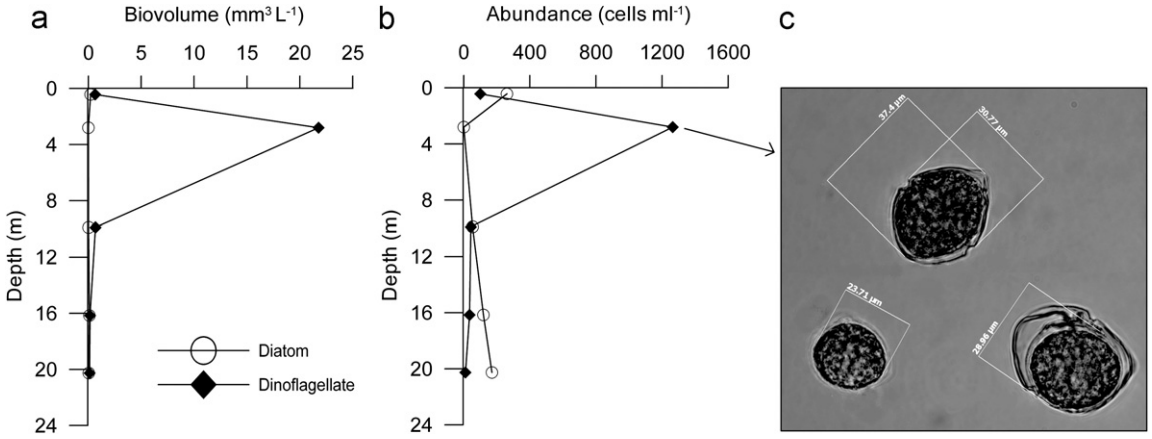

Fig. 6. Diatom and dinoflagellates at inner-fjord Station P3: (a) biovolume, (b) abundance, (c) illustration of the blooming organism (*Scrippsiella* sp.) at ~3 m depth.

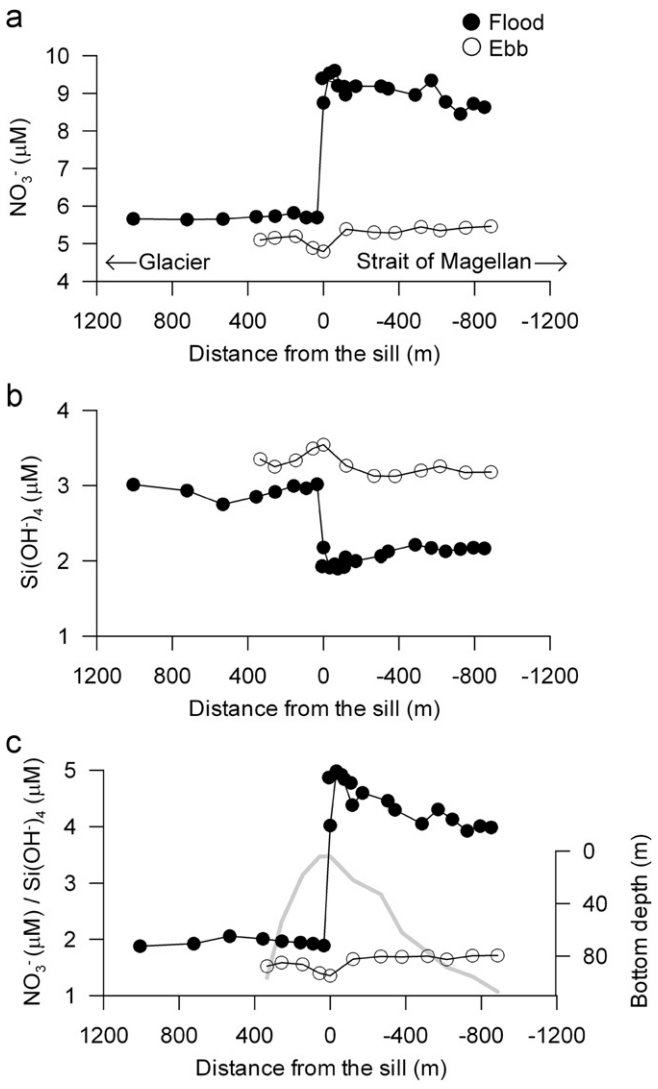

Fig. 7. Nitrate and DSi concentrations in surface waters over the Seno Ballena sill during flooding and ebbing in December 2007. The thick line in figure c depicts the bottom depth (note that the secondary *y*-axis is inverted for a better depiction of the sill location).

The surface DSi concentration varied inversely with surface nitrate (Fig. 7). This pattern probably resulted from the mixing between sea (salty, nitrate-rich, silicate-poor) and continental (fresh, nitrate-poor, silicate-rich) waters (Frangópulos et al., 2007). The aspirated marine waters that entered the inner-fjord during flood were dense, nitrate-rich, and DSi-poor (see Figs. 2 and 7), unlike the water leaving the inner-fjord during ebb, which was less dense, nitrate-poor, and DSi-rich. The reduction in nitrate during ebb was probably caused by uptake from primary production (see estimation of new productivity in Section 4.2), which appeared to be particularly active in the surface layer of this fjord. Note that the supersaturated DO levels (Fig. 3) may have indicated net primary productivity, consistent with the concentration of photosynthetic pigments on the top 4-m layer (Fig. 4). The small increment in DSi within the inner-fjord during ebb was most probably caused by the input of continental water, typically enriched in silicate (see Section 4.3).

During flood, the high NO_3^-:DSi ratio (Fig. 7c) of the waters aspirated into the fjord was consistent with the silicate and nitrate levels of the subpycnocline waters during ebb (see DSi levels at St. P1; Fig. 4), i.e., low subpycnocline DSi levels as compared to nitrate levels.

A deeper silicate-cline (compared to the nitrate-cline) is not a rare occurrence in Patagonian waters (e.g., see data report from the 1967 Scorpio Expedition, Nierenberg and Fye, 1969) or in other high-latitude systems (e.g., Barents Sea, Rey and Skjoldal, 1987). Rey and Skjoldal (1987) suggested that deep silicic acid consumption results in a vertical separation of the silicic acid gradient (silicocline) from the nitracline. Early spring diatom blooms (typically dominated by chain diatoms, e.g., Iriarte et al., 2001) could preferentially remove silicate from the water column, e.g., through the production/export of heavily silicificated resistant spores (Rey and Skjoldal, 1987) and/or because silicic acid uptake by diatoms can exceed the depth at which nitrogen assimilation takes place (Nelson and Goering, 1978). Indeed, N and Si metabolisms in diatoms are not coupled (Martin-Jézéquel et al., 2000). Additionally, Subantarctic Mode Water (SAMW) that deeply influences the surface waters of the entire Patagonia has conspicuously high concentrations of nitrate compared to DSi (Sarmiento et al., 2003).

Regardless of its origin, a particularly deep silicocline may prevent re-fertilization through relatively shallow upwelling, consequently discouraging further diatom growth due to reduced upward transport (Rey and Skjoldal, 1987). It is worth noting that the silicate available in the entire water column was low (see Fig. 4), whereas previous observations of the streams that flow into Seno Ballena have shown relatively high DSi levels (up to 22 µM $Si(OH)_4$; Frangópulos et al., 2007) compared to surface fjord waters (typically 2–3 µM; Fig. 4). Despite minimal DSi enrichment of inner-fjord surface waters (see Fig. 7b), a relative maximum could still be observed over the sill (two observations,

Table 1
Correlation between the concentration of nitrate (or DSi) and the distance from the sill at which the sample was collected, in two strata: (a) Flood/Ebb and (b) inner/outer fjord location.

	Flood inner fjord side	Flood outer fjord side	Ebb inner fjord side	Ebb outer fjord side
Correlation (R) Nitrate-distance from the sill	($p=0.1$, $n=8$)	$R=-0.8$ ($p<0.05$, $n=14$)	($p=0.4$, $n=4$)	($p=0.2$, $n=7$)
Correlation (R) DSi-distance from the sill	($p=0.8$, $n=8$)	$R=+0.9$ ($p<0.05$, $n=14$)	($p=0.4$, $n=4$)	($p=0.4$, $n=7$)

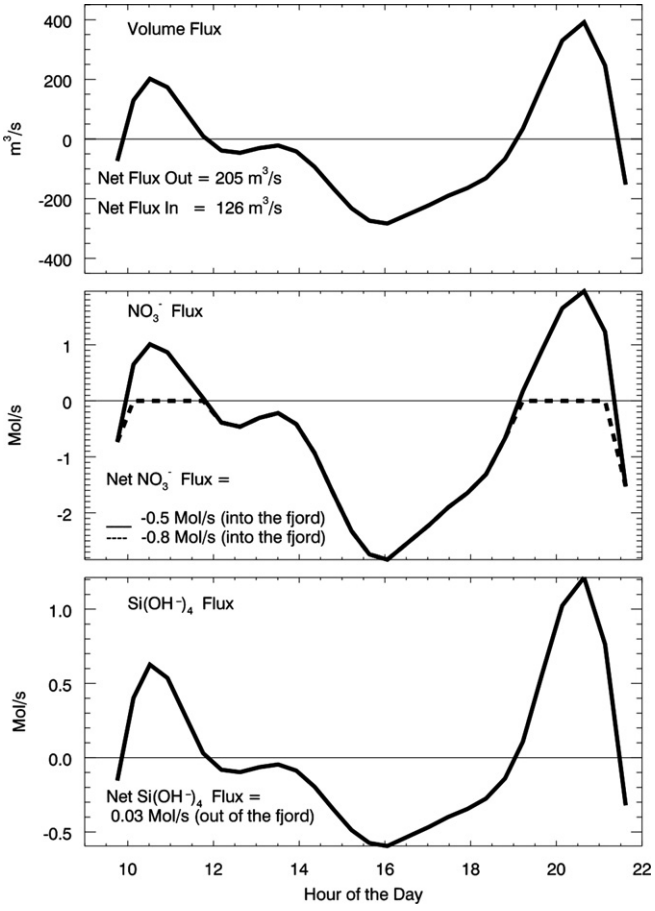

Fig. 8. Flux of water volume, nitrate, and DSi at the Seno Ballena's sill during a tidal cycle. Current data used to estimate fluxes were obtained in December 2003.

Fig. 7b). Most likely, this local maximum was indicating a convergence of low salinity water (and, consequently, silicate-rich, nitrate-poor) near the sill during ebbing (Fig. 3) (Valle-Levinson et al., 2006). Moreover, the relative warmth of the low salinity water at Station 3 (Fig. 3) suggested that the surface water came from continental streams rather than more direct meltwater from the glacial tip. Low salinity surface water near the glacier was particularly cold (Fig. 2a–b).

4.2. New productivity estimated from nitrate mass balance

The primary productivity supported by the net nitrate flux, which was –0.5 moles s^{-1} toward the inner-fjord area ($\sim$8 km^2), was estimated to be $\sim$0.4 g C day^{-1} m^{-2}. This estimate was obtained assuming that the generated phytoplankton biomass had a Redfield carbon/nitrogen atomic ratio (106:16). The estimate of 0.4 g C day^{-1} m^{-2} for mean new productivity (P_{New}) of the inner fjord represents 62% of its potential P_{New}. The P_{New} required to drive complete nitrate depletion at the inner-fjord ($\sim$0.6 g C day^{-1} m^{-2}) corresponded to a net nitrate flux of –0.8 moles s^{-1} (see Section 3.3). This potential P_{New} is set by the interplay of the periodic nitrate fertilization of the inner fjord during flooding and the dilution caused by virtually nitrate-free freshwater inputs (Frangópulos et al., 2007). Both actual ($\sim$0.4 g C day^{-1} m^{-2}) and potential ($\sim$0.6 g C day^{-1} m^{-2}) estimates of P_{New} were lower than primary productivity estimates for this region in austral spring (3 ± 3 g C day^{-1} m^{-2}; Pizarro et al., 2005). The high productivity reported by Pizarro et al. (2005) for austral spring was obtained when chain diatoms dominated the phytoplankton assembly (Pizarro et al., 2005). We suggest that the low productivity levels reported here respond mainly to (1) a post-bloom condition, in which low levels of DSi preclude diatom blooms (see Sections 4.1) and (2) an inner fjord phytoplankton assemblage unable to rapidly deplete nitrate in surface waters. The ability of photosynthetic picoplankton to consume nitrate is expected to be low compared to micro-phytoplankton-dominated systems. Indeed, small-sized phytoplankton can be ammonium supported (Jochem, 1989). The prevalence of picoplankton in the upper layer of the inner fjord was probably not related to nitrate availability but to the picoplankton's ability to live in low-light environments (e.g., Bricaud et al., 1995) such as the silt-turbid inner fjord.

4.3. Freshwater and DSi inputs

Surface water DSi was low in the entire survey but slightly higher when waters were leaving the inner fjord during ebb (Fig. 7). This enrichment of the inner fjord leads to a flux of $\sim$0.03 moles s^{-1} toward the ocean that can be explained by DSi in the freshwater inputs ($R=80$ m^3 s^{-1}, see Section 3.3). We estimated a minimum DSi concentration for freshwater inputs of 0.4 μM by assuming that no consumption of DSi occurs in the inner fjord. Although we have no direct measurements of the freshwater discharged to this fjord, the salinity gradients along the fjord suggest that most of the freshwater inputs to Seno Ballena occur at the fjord head, where the most plausible freshwater source is sub-glacial melting. Because DSi concentration of surface water was particularly low at the fjord head (<2 μM, see St. P4 in Fig. 4), we also expect a low DSi concentration for the submarine discharge (i.e. <2 μM). This value is certainly not far from the minimum DSi concentration estimated previously (0.4 μM). Frangópulos et al. (2007) reported higher DSi concentrations (19–24 μM DSi) in two small watersheds (2 L s^{-1}) sampled in November 2006 in the central area of Seno Ballena. Other observations of a small waterfall ($\sim$20 L s^{-1}) entering the inner-fjord were made during a December 2003 expedition and showed low DSi concentrations (1–2 μM, M. Frangopulos, unpublished data). These values point out the potential variability of DSi concentrations, which range from low (1 μM) to moderate (24 μM), for small continental sources. However, since these small streams most likely constitute a small fraction of freshwater input, we do not expect a large DSi contribution here, either. The weathering and subsequent loading

of bioavailable silicate (including DSi, opal, and amorphous silica) to coastal areas is a function of lithology, vegetation cover, precipitation, and temperature (Conley et al., 2006; Humborg et al., 2006a). The granitic lithology of the region may result in moderate to high levels of DSi loading from weathering (Berner, 2004). However, as in other periglacial areas (Drever and Zobrist, 1992; Kelly et al., 1998; Anderson et al., 2000; Humborg et al., 2004; Anderson, 2007), in this study area, the coastal terrain's steep slopes (resulting in small catchment areas), high proportion of runoff, limited soil, and poor development of vascular vegetation seem to result in low levels of DSi in the incoming freshwater.

4.4. High nitrate:silicate ratios in fjord waters and possible effects for the micro-phytoplankton community

Despite enriched DSi in the surface inner-fjord waters, the DSi concentration was lower than that of nitrate, not only in the low-salinity surface waters but also at every depth sampled (Figs. 4 and 7). Assuming a 1:1 silicate:nitrogen diatom biomass ratio (Brzezinkski, 1985), the original low DSi:nitrate ratio of the aspirated water (1:5, Fig. 7c) should lead to silicate limitations for diatom growth (Turner et al., 1998). Indeed, silicate levels throughout the water column were so low (mostly 2–3 μM) that they may have ceased to stimulate the dominance of diatomaceous phytoplankton (Egge and Aksnes, 1992). Officer and Ryther (1980) suggested that a shift in the Si:N atomic ratio from above 1:1 to below 1:1 would increase the proportion of flagellate algae, including those that produce harmful algal blooms. Consistent with that, dinoflagellates were responsible for the largest peaks of chlorophyll in the nitrate-rich (5–10 μM NO_3^-), DSi-poor (<2 μM $Si(OH)_4$) waters that characterized the inner-fjord (Figs. 4 and 6). The vertical mobility of dinoflagellates might allow them to remain at the base of the halocline, preventing or reducing their advection out of the inner-fjord (Goebel et al., 2005). This possibility, plus high nitrate, the high nitrate:silicate ratio, and the availability of light at the base of the shallow halocline provided the conditions for dinoflagellate proliferation. The dinoflagellate *Scrippsiella* sp. that bloomed at Station P3 (1265 cel mL^{-1}; see Fig. 6) is a common inhabitant of Magellanic fjords (Uribe and Ruiz, 2001; Alves-de-Souza et al., 2008b) found particularly in areas of high stratification (Alves-de-Souza et al., 2008a). This organism has also been reported to form red tides off the coast of Chile (Muñoz and Avaria, 1983).

A previous study in this fjord (November 2006; Frangópulos et al., 2007) showed a similar pattern near Station P3: a dinoflagellate bloom (in that case, 16,500 cel mL^{-1} of *Alexandrium ostenfeldii*; see Hansen et al., 1992) occurred at 5 m depth and was associated with high levels of Chl-a (7 mg m^{-3}), high nitrate (7 μM), and low DSi (3 μM). We suggest that this is a recurrent pattern of micro-phytoplankton composition within the inner fjord area of Seno Ballena and could be triggered by the high nitrate: DSi ratio of the water entering the inner-fjord during flood.

The high nitrate, low DSi of the waters entering the inner-fjord implied that an eventual diatom dominance in this inner-fjord system would be critically dependent on terrestrial silicate inputs, as in other fjords that receive silicate-enriched freshwater (e.g., Doubtful Sound, New Zealand; Goebel et al., 2005).

We suggest that the combination of a high NO_3^-:DSi ratio in the waters entering the inner fjord and an insufficient influx of bioavailable silicate of terrestrial origins, prevents diatom proliferations. Consequently, other phytoplankton groups can bloom in the nutrient-replete, well-stratified inner waters of Seno Ballena. Hence, any rise in the NO_3^-:DSi ratios in fjords highly susceptible to silicate limitation such as Seno Ballena may enhance the frequency and/or intensity of non-diatomaceous blooms. This has important ecological and social implications for current and future impacts from anthropogenic activity on Patagonian waters.

The NO_3^-:DSi ratio of Patagonian waters is expected to rise in the future due to a rapid increment of anthropogenic activity. Nitrogen inputs to the coastal ocean are expected to augment due to salmon farming (e.g., Aure and Stigebrandt, 1990; Troell et al., 1997; Iriarte et al., 2007; Sanderson et al., 2008) or other anthropogenic perturbations (e.g., urbanization, agriculture, industrial activities; see Turner et al., 2003), whereas land-sea fluxes of bioavailable silica are expected to decrease through dam construction (e.g., Humborg et al., 1997; Conley et al., 2000; Humborg et al., 2006b; Ragueneau et al., 2006). We are also likely to see indirect anthropogenic effects on biogeochemical cycling mediated by climate change in terms of relative nutrient inputs via changes in precipitation and temperature. The prediction of reduced austral summer precipitation in southern Chile during this century (CONAMA, 2006) could, therefore, result in reduced DSi fluxes to the coastal ocean.

5. Conclusions

1. Tidal circulation–topographic interactions, terrestrial DSi inputs, and local productivity were relevant factors for determining the temporal and spatial variability of nitrate and DSi in Seno Ballena in December 2007.
2. The high NO_3^-:DSi ratio of the waters entering the inner-fjord of Seno Ballena could be the key factor explaining non-diatomaceous blooms in the inner portion of this fjord in austral summer.

Acknowledgements

We thank Sebastian Vidal, Oscar Mancilla, Carlos Olave, and Juan San Martin for helping with field work. We thank two anonymous reviewers for their valuable suggestions. This study was funded by the Centro de Estudios del Cuaternario Fuego-Patagonia (CEQUA).

References

Allen, J.T., Brown, L., Sanders, R., Moore, C.M., Mustard, A., Fielding, S., Lucas, M., Rixen, M., Savidge, G., Henson, S., Mayor, D., 2005. Diatom carbon export enhanced by silicate upwelling in the northeast Atlantic. Nature 437, 728–732.

Alves-de-Souza, C., González, M.T., Iriarte, J.L., 2008a. Functional groups in marine phytoplankton assemblages dominated by diatoms in fjords of southern Chile. J. Plankton Res. 30, 1233–1243.

Alves-de-Souza, C., Varela, D., Navarrete, P., Fernández, P., Leal, P., 2008b. Distribution, abundance and diversity of modern dinoflagellate cyst assemblages for southern Chile (43–54°S). Bot. Mar. 51, 399–410.

Anderson, S.P., 2007. Biogeochemistry of Glacial Landscape System. Annu. Rev. Earth Pl. Sci. 35, 375–399.

Anderson, S.P., Drever, J.I., Frost, C.D., Holden, P., 2000. Chemical weathering in the foreland of a retreating glacier. Geochim. Cosmochim. Acta 64, 1173–1189.

Antezana, T., Hamamé, M., 1999. Short-term changes in the plankton of a highly homogeneous basin of the Strait of Magellan (Paso Ancho) during spring 1994. Sci. Mar. 63, 59–67.

Antezana, T., Guglielmo, L., Ghirardelli, E., 1992. Microbasins within the Strait of Magellan affecting zooplankton distribution. In: Gallardo, V.A., Ferreti, O., Moyano, H.I. (Eds.), Oceanografía en Antártica. Ediciones Documentas, Santiago, pp. 453–458.

Aure, J., Stigebrandt, A., 1990. Quantitative estimates of the eutrophication effects of fish farming on fjords. Aquaculture 90, 135–156.

Berner, R.A., 2004. The Phanerozoic Carbon Cycle: CO_2 and O_2. Oxford University Press , 159p.

Braun, M., Blanco, J.L., Osses, J., 1993. Programa básico de monitoreo de marea roja en la XII región. Informe Técnico presentado a la Subsecretaría de Pesca por el Instituto de Fomento Pesquero. July 1993. 181 pp, unpublished manuscript.

Bricaud, A., Babin, M., Morel, A., Claustre, H., 1995. Variability in the chlorophyll-specific absorption coefficients of natural phytoplankton: analysis and parameterization. J. Geophys. Res. 100 (C7), 13321–13332.
Brzezinkski, M.A., 1985. The Si:C:N ratio of marine diatoms: interspecific variability and the effect of some environmental variables. J. Phycol. 21, 347–357.
Catalano, G., Acuña, A., Benedetti, F., 1996. The Strait of Magellan dissolved oxygen and nutrients during the 2nd joint Italian–Chilean Cruise (March 1995). In: Faranda, F.M., Guglielmo, L., Povero, P. (Eds.), National Programme Antarctic Research Strait of Magellan Ocean. Cruise March–April 1995, pp. 53–68.
Clément, A., Guzmán, L., 1989. Red tides in Chilean fjords. In: Okaichi, T., Anderson, D.M., Nemoto, T. (Eds.), Red Tides: Biology, Environmental Sciences and Toxicology. Elsevier, New York, pp. 121–124.
Cokelet, E.D., Jenkins, A.J., Etherington, L.L., 2007. A transect of Glacier Bay ocean currents measured by acoustic Doppler current profiler (ADCP), in: Piatt, J.F., Gende, S.M. (Eds.), Proceedings of the Fourth Glacier Bay Science Symposium, October 26–28, 2004: U.S. Geological Survey Scientific Investigations Report 2007–5047, pp. 80–83.
CONAMA, 2006. Estudio de la variabilidad climática en Chile para el Siglo XXI, Informe Final presentado a CONAMA por la Universidad de Chile, 63 pp, unpublished manuscript.
Conley, D.J., Schelske, C.L., Stoermer, E.F., 1993. Modification of the biogeochemical cycle of silica with eutrophication. Mar. Ecol. Prog. Ser. 101, 179–192.
Conley, D.J., Stålnacke, P., Pitkänen, H., Wilander, A., 2000. The transport and retention of dissolved silicate by rivers in Sweden and Finland. Limnol. Oceanogr. 45, 1850–1853.
Conley, D.J., Sommer, M., Meunier, J.D., Kaczorek, D., Saccone, L., 2006. Silicon in the Terrestrial Biosphere. In: Ittekkot, V., Unger, D., Humborg, C., An, N.T. (Eds.), The Silicon Cycle: Human Perturbations and Impact on Aquatic Systems. Island Press, Washington, D.C.
Dávila, P.M., Figueroa, D., Müller, E., 2002. Freshwater input into the coastal ocean and its relation with the salinity distribution off austral Chile (35–55°S). Cont. Shelf Res. 22, 521–534.
Dickson A.G., 1995. Determination of dissolved oxygen in sea water by Winkler titration. WOCE Operations Manual. Part 3.1.3 Operations & Methods, WHP Office Report WHPO 91–1. unpublished manuscript.
Drever, J.I., Zobrist, J., 1992. Chemical weathering of silicate rocks as a function of elevation in the southern Swiss Alps. Geochim. Cosmochim. Acta 56, 3209–3216.
Egge, J.K., Aksnes, D.L., 1992. Silicate as regulating nutrient in phytoplankton competition. Mar. Ecol. Prog. Ser. 83, 281–289.
Frangópulos, M., Blanco, J.L., Hamamé, M., Rosales, S., Torres, R., Valle-Levinson, A., 2007. Análisis y diagnóstico de las principales características oceanográficas del área marina costera protegida Francisco Coloane, Informe Final Proyecto GEF-PNUD "Conservación de la Biodiversidad de Importancia Mundial a lo Largo de la Costa Chilena" November 2007, 122 pp. unpublished manuscript.
Goebel, N.L., Wing, S.R., Boyd, P.W., 2005. A mechanism for onset of diatoms blooms in a fjord with persistent salinity stratification. Estuar. Coast. Shelf Sci. 64, 546–560.
Hamamé, M., Antezana, T., 1999. Chlorophyll and zooplankton in microbasins along the Straits of the Magellan-Beagle Channel passage. Sci. Mar. 63 (Supl. 1), 35–42.
Hansen, P.J., Cembella, A.D., Moestrup, Ø., 1992. The marine dinoflagellate *Alexandrium ostenfeldii*: paralytic shellfish toxin concentration, composition, and toxicity to a tintinnid ciliate. J. Phycol. 28, 597–603.
Holmedal, L.E., Utnes, T., 2006. Physical–biological interactions and their effect on phytoplankton blooms in fjords and near-coastal waters. J. Mar. Res. 64, 97–122.
Humborg, C., Ittekkot, V., Cociasu, A., Bodungen, B.V., 1997. Effect of Danube River Dam on Black Sea biogeochemistry and ecosystem structure. Nature 386, 385–388.
Humborg, C., Smedberg, E., Blomqvist, S., Mörth, C.M., Brink, J., Rahm, L., Danielsson, A., Sahlberg, J., 2004. Nutrient variations in boreal and subartic swedish rivers: landscape control of land sea fluxes. Limnol. Oceanogr. 49, 1871–1883.
Humborg, C., Rahm, L., Smedberg, E., Morth, C., Danielsson, A., 2006a. Dissolved silica dynamics in boreal and arctic rivers: vegetation control over temperature?. In: Ittekkot V., Unger, D., Humborg, C., An, N.T. (Eds.), The Silicon Cycle: Human Perturbations and Impact on Aquatic Systems. Island Press, Washington, DC.
Humborg, C., Pastuszak, M., Aigars, Juris, Siegmund, H., Mörth, C.-M., Ittekkot, V., 2006b. Decreased silica land–sea fluxes through damming in the baltic sea catchment – significance of particle trapping and hydrological alterations. Biogeochemistry 77, 265–281.
Huygens, D., Boeckx, P., Templer, P., Paulino, L., Van Cleemput, O., Oyarzún, C., Müller, C., Godoy, R., 2008. Mechanisms for retention of bioavailable nitrogen in volcanic rainforest soils. Nat. Geosci. 1 (8), 543–548.
Iriarte, J.L., Uribe, J.C., Valladares, C., 1993. Biomass of size fractionated phytoplankton during the spring–summer season in Southern Chile. Bot. Mar. 36, 443–450.
Iriarte, J.L., Kusch, A., Osses, J., Ruiz, M., 2001. Phytoplankton biomass in the sub-antarctic area of the Straits of Magellan (53°S), Chile during spring–summer 1997/1998. Polar Biol. 24, 154–162.
Iriarte, J.L., González, H.E., Liu, K.K., Rivas, C., Valenzuela, C., 2007. Spatial and temporal variability of chlorophyll and primary productivity in surface waters of southern Chile (41.5–43°S). Estuar. Coast. Shelf Sci. 74, 471–480.
Jochem, F., 1989. Distribution and importance of autotrophic ultraplankton in a boreal inshore area (Kiel Bight, Western Baltic). Mar. Ecol. Prog. Ser. 53, 153–168.
Kelly, E.F., Chadwick, O.A., Hilinski, T.E., 1998. The effect of plants on mineral weathering. Biogeochemistry 42, 21–53.
Largier, J.L., 1992. Tidal intrusion fronts. Estuaries 15, 26–39.
Magazzù, G., Panella, S., Decembrini, F., 1996. Seasonal variability of fractionated phytoplankton, biomass and primary production in the Strait of Magellan. J. Mar. Syst. 9, 249–267.
Martin-Jézéquel, V., Hildebrand, M., Brzezinski, M.A., 2000. Silicon metabolism in diatoms: implications for growth. J. Phycol. 36, 821–840.
Mann, K.H., Lazier, J.R.N., 1996. Dynamics of Marine ecosystem, Biological–Physical Interactions in the Ocean Second edition Blackwell Science, Boston.
Molinet, C., Lafon, A., Lembeye, G., Moreno, C., 2003. Patrones de distribución espacial y temporal de floraciones de Alexandrium catenella (Whedon and Kofoid) Balech 1985, en aguas interiores de la Patagonia noroccidental de Chile. Rev. Chil. Hist. Nat. 76, 681–698.
Muñoz, P., Avaria, S., 1983. *Scrippsiella trochoidea* (Stein) Loeblich, Nuevo organismo causante de marea roja en la bahía de Valparaíso, Chile. Rev. Biol. Mar. Valparaíso, Chile 19 (1), 63–78.
Murray, C.N., Riley, J.P., 1969. The solubility of gases in distilled water and seawater – II. Oxygen. Deep-Sea Res. 16, 311–320.
Nelson, D.M., Goering, J.J., 1978. Assimilation of silicic acid by phytoplankton in Baja California and northwest Africa upwelling systems. Limnol. Oceanogr. 23, 508–517.
Nierenberg, W.A., Fye, P.M., 1969. Physical and chemical data from the Scorpio expedition in the south pacific ocean aboard USNS ELTANIN cruise 28 and 29, 12 March–31 July 1967. WHOI Reference 69-56.
O'Donnell, J., 1993. Surface fronts in estuaries: a review. Estuaries 16, 12–39.
Officer, C.B., Ryther, J.H., 1980. The possible importance of silicon in marine eutrophication. Mar. Ecol.—Prog. Ser 3, 83–91.
Olenina, I., Hajdu, S., Edler, L., Andersson, A., Wasmund, N., Busch, S., Göbel, J., Gromisz, S., Huseby, S., Huttunen, M., Jaanus, A., Kokkonen, P., Ledaine, I., Niemkiewicz, E., 2006. Biovolumes and size-classes of phytoplankton in the Baltic Sea. HELCOM Balt. Sea Environ. Proc. 106, 144.
Parsons, T., Maita, Y., Lalli, C., 1984. A Manual of Chemical and Biological Methods for Seawater Analysis. Pergamon Press, UK 169.
Perakis, S.S., Hedin, L.O., 2002. Nitrogen loss from unpolluted South American forests mainly via dissolved organic compounds. Nature 415, 416–419.
Perillo, G., 1995. Definitions and geomorphologic classifications of estuaries. In: Perillo, G. (Ed.), Geomorphology and Sedimentology of Estuaries. Developments in Sedimentology, vol. 53, pp. 17–47.
Pizarro, G., Montecino, V., Guzmán, L., Muñoz, V., Chacón, V., Pacheco, H., Frangópulos, M., Retamal, L., Alarcón, C., 2005. Patrones locales recurrentes del fitoplancton en fiordos y canales australes (43°–56°S) en primavera y verano. Cienc. Tecnol. Mar. 28 (2), 63–83.
Ragueneau, O., Conley, D.J., Leynaert, A., Longphuirt, S., Slomp, C., 2006. Responses of coastal ecosystems to anthropogenic perturbations of silicon cycling. In: Ittekkot, V., Unger, D., Humborg, C., An, N.T. (Eds.), The Silicon Cycle: Human Perturbations and Impact on Aquatic Systems. Island Press, Washington, DC.
Rey, F., Skjoldal, H.R., 1987. Consumption of silicic acid below the euphotic zone by sedimenting diatom blooms in the Barents Sea. Mar. Ecol.—Prog. Ser. 36, 307–312.
Saggiomo, V., Goffart, A., Carrada, G.C., Hecq, J.H., 1994. Spatial patterns of phytoplanktonic pigments and primary production in a semi-enclosed periantarctic ecosystem: the Strait of Magellan. J. Mar. Syst. 5, 119–142.
Sanderson, J.C., Cromey, C.J., Dring, M.J., Kelly, M.S., 2008. Distribution of nutrients for seaweed cultivation around salmon cages at farm sites in north-west Scotland. Aquaculture 278, 60–68.
Sarmiento, J.L., Gruber, N., Brzezinski, M.A., Dunne, J.P., 2003. High-latitude controls of thermocline nutrients and low latitude biological productivity. Nature 427, 56–60.
Seim, H.E., Gregg, M.C., 1997. The importance of aspiration and channel curvature in producing strong vertical mixing over the sill. J. Geophys. Res. 102, 3451–3472.
Servicio Nacional de Geología y Minería, 2003. Mapa Geológico de Chile: Version Digital. No. 4, CD ROM Versión 1.0. Gobierno de Chile.
Silva, N., Calvete, C., 2002. Características oceanográficas físicas y químicas de canales australes chilenos entre el Golfo de penas y el Estrecho de Magallanes (Crucero CIMAR-Fiordo 2). Cienc. Tecnol. Mar 25, 23–88.
Silva, N., Guzman, D., 2006. Condiciones oceanográficas fisicas y químicas, entre boca del Guafo y fiordo Aysén (crucero CIMAR 7 Fiordos). Cienc. Tecnol. Mar 29, 25–44.
Silva, N., Valdenegro, A., 2008. Caracterización oceanográfica de canales australes chilenos entre la Boca del Guafo y los canales Pulluche-Chacabuco (CIMAR 8 Fiordos). Cienc. Tecnol. Mar 31, 05–44.
Stommel, H., Bryden, H., Mandelsdorf, P., 1973. Does some of the mediterranean outflow come from great depth? Pure Appl. Geophys. 105 879–899.
Strickland, J.D.H., Parsons, T.R., 1968. A Practical Handbook of Seawater Analysis. Bull. Fish Res. Board Can. 167.
Troell, M., Halling, C., Nilsson, A., Buschmann, A.H., Kautsky, N., Kautsky, L., 1997. Integrated marine cultivation of *Gracilaria chilensis* (Gracilariales, Rhodophyta) and salmon cages for reduced environmental impact and increased economic output. Aquaculture 156, 45–61.
Turner, E.R., Qureshi, N., Rabalais, N.N., Dortch, Q., Justic, D., Shaw, R.F., Cope, J., 1998. Fluctuating silicate:nitrate ratios and coastal plankton food webs. Proc. Natl. Acad. Sci. USA 95, 13048–13051.
Turner, E.R., Rabalais, N.N., Justic, D., Dortch, Q., 2003. Future aquatic nutrient limitations. Mar. Pollut. Bull. 46, 1032–1034.

Uribe, J.C., 1992. Fitoplancton en los fiordos magallánicos. In: Gallardo, V.A., Ferreti, O., Moyano, H.I. (Eds.), Oceanografía en Antártica. Ediciones Documentas, Santiago, pp. 467–478.
Uribe, J.C., Ruiz, M., 2001. Gymnodinium brown tide in the magellanic fjords, Southern Chile. Rev. Biol. Mar. Oceanog. 36 (2), 155–164.
Utermöhl, H., 1958. Vervollkommnung der quantitativen phytoplankton-methodik. Mitteilungen Int. Ver. Theor. Ang. Limnol. 9, 1–38.
Valle-Levinson, A., Blanco, J.L., Frangópulos, M., 2006. Hydrography and frontogenesis in a glacial fjord off the Strait of Magellan. Ocean Dynam. 56, 217–227.
Valle-Levinson, A., Blanco, J.L., Frangopulos, M., 2007. Depth-dependent overtides from internal tide reflection in a glacial fjord. Estuar. Coasts 30, 127–136.
Vanucci, S., Mangoni, O., 1999. Pico- and nanophytoplankton assemblages in a subantartic ecosystem: the Strait of Magellan. Bot. Mar. 42, 563–572.
Vargas, C.A., Martinez, R.A., San Martin, V., Aguayo, M., Silva, N., Torres, R., this issue. Allochthonous subsidies of organic matter across a lake-river-fjord landscape in the Chilean Patagonia: implications for marine zooplankton in inner fjord areas. Cont. Shelf Res. doi:10.1016/j.csr.2010.06.016.